J Mater Sci (2010) 45:5960–5966
DOI 10.1007/s10853-010-4681-3

Prediction of no-recrystallization temperature by simulation of multi-pass flow stress curves from single-pass curves

Soheil Solhjoo · R. Ebrahimi

Received: 13 January 2010 / Accepted: 29 May 2010 / Published online: 15 June 2010

Abstract In this investigation an algorithm is given to simulate the flow stress curves for multi-pass hot deformation processes simply from the data obtained from single-pass hot torsion test. Using the obtained multi-pass curves the value of no-recrystallization temperature (T_{nr}) is calculated. This method is examined on a Nb-microalloyed steel. Maximum error in calculation of T_{nr} with this method and the values obtained from empirical tests was 1.5% which is a very low value. The predicted results are found to be in accord with the experimental data.

Abbreviations

DRX	Dynamic recrystallization
T_{nr}	No-recrystallization temperature
MFS	Mean flow stress
SRX	Static recrystallization
MDRX	Metadynamic recrystallization

Introduction

Many researchers have worked on thermo-mechanical behavior of low carbon Nb-microalloyed steels. In fact, most hot rolled microalloyed steels contain niobium, since this element presents the advantage in comparison with vanadium of being less soluble in austenite at temperatures usually used in hot rolling [1]. The appropriate employment of microalloying elements in high strength low alloy (HSLA) steels, coupled with thermo-mechanical processing, can provide improvements in both strength and toughness [2–5]. This is achieved by suitable combination of the recrystallization and precipitation phenomena that take place during hot deformation. The interaction between deformation, recrystallization, and precipitation results the no-recrystallization temperature (T_{nr}), defined as the temperature at which recrystallization starts to be inhibited.

The determination of the T_{nr} is a crucial step in designing controlled rolling schedules, because it determines the temperature below which strain is accumulated in the austenite (pancaking). If the final passes of rolling take place at temperatures below T_{nr} the deformed austenite grains should contain a greater density of dislocations, which would be potential sites for ferrite nucleation, leading to the ferrite grains developed after the transformation would be much finer, thus improving mechanical properties [6].

The T_{nr} is a function of composition, effective strain applied in each pass, strain rate, inter-pass time (t_{ip}), and reheating temperature (T_{rh}) [1, 7, 8]. An increase in the T_{nr} allows finish rolling to be conducted at higher temperatures, which in turn enable lower loads to be developed or larger reductions to be applied without consuming additional energy. T_{nr} could be determined from rolling mill log data [9], but the most common method for determining T_{nr} consists of simulating successive rolling passes and then graphically representing the mean flow stress (MFS) versus the inverse of the absolute temperature for each of the simulated passes [10–16]. Determination of MFS requires the knowledge of flow stress behavior of the metal in each

S. Solhjoo (✉)
Department of Materials Science and Engineering, Sharif University of Technology, Azadi Ave., Tehran, Iran
e-mail: soheilsolhjoo@yahoo.com

R. Ebrahimi
Department of Materials Science and Engineering, School of Engineering, Shiraz University, Zand Ave., Shiraz, Iran
e-mail: ebrahimy@shirazu.ac.ir

pass and can be obtained from hot rolling experiments. Since multi-pass hot rolling testing is hard to control, multi-pass hot torsion testing can be used as a powerful tool for simulations of actual industrial hot rolling schedules [17]. Experimental tests in order to measure the flow stress of alloys at different loading conditions, i.e., various strain rates and temperatures are necessary but very expensive and time consuming. Therefore, many researchers tried to mathematically model the stress–strain curves for different alloys to predict the flow stress curves under different forming conditions.

In this paper the isothermal models used for the modeling of microstructural evolution during hot rolling of Nb-microalloyed steels are briefly described. Then an algorithm is proposed and used to simulate the multi-pass flow stress curves in hot rolling schedules from the single-pass hot torsion curves. Using the behavior of the steel during each schedule the MFS for each pass is calculated and then the MFS plotted verses the inverse of the absolute temperature for each of the simulated passes. Then the values of T_{nr} are estimated. Finally, the effect of strain rate in each pass on the value of T_{nr} is studied. The results are found to be in an excellence agreement with empirical data.

Microstructural evolution models

During a particular pass of a hot rolling schedule, the effective strain will determine which softening mechanism will operate, static recrystallization (SRX) or dynamic and metadynamic recrystallization (DRX + MDRX). Depending on the type of softening, different equations are then employed to specify the grain size and fractional softening. Over the years, several research groups have developed equations relating the evolution of austenite grain size (d_γ) to the hot rolling parameters. A softening model uses parameters such as strain, strain rate, initial grain size, and temperature to decide upon the mechanism and calculate the extent of softening. The model describing kinetics of SRX and MDRX is based on the modified Avrami equation, as proposed by Sellars [18], which generally is used as:

$$X = 1 - \exp\left[-0.693\left(\frac{t_{RX}}{t_{0.5,RX}}\right)^K\right] \quad (1)$$

where X is recrystallized fraction between two passes, t_{RX} is the time which the metal has for recrystallization, $t_{0.5,RX}$ is the time for 50% recrystallization, and K is the Avrami exponent depends on whether the softening is by SRX or MDRX [19]. But in the case of Nb-microalloyed steels, K is reported to be 1 in both SRX [20] and MDRX [21, 22] conditions. The value of $t_{0.5}$ depends on whether the softening is by SRX ($t_{0.5,SRX}$) or MDRX ($t_{0.5,MDRX}$). In order to find which softening mechanism operates, the critical strain required to initiate DRX would be calculated using the relation [23]:

$$\varepsilon_C = A \cdot \varepsilon_P \quad (2)$$

where ε_C and ε_P are the critical and peak strain, respectively and A is a material constant. Siciliano and Jonas showed that constant A can be described as a function of effective Nb concentration [5]. Recently Xu et al. [24] showed that their suggested equation is only available to the relatively low Nb contents, i.e., smaller than 0.06%. A new fit equation capable of being applied over wider range of Nb content (up to 0.1%) is given as [24]:

$$A = 0.8 - 10.8[Nb_{eff}] + 64.4[Nb_{eff}]^2 \quad (3)$$

where Nb_{eff} is specified by [5, 24]:

$$Nb_{eff} = Nb - \frac{Mn}{120} + \frac{Si}{94} \quad (4)$$

Considering the composition of the Nb-microalloyed which is investigated in this work (see "Experimental procedure" section) and Eq. 4, the value of Nb_{eff} is obtained to be 0.027.

The peak strain equation is derived by Roucoules [25] and improved by Minami et al. [26]. In order to improve the results, the concentration of Nb in the peak strain equation is replaced by effective Nb concentration.

$$\varepsilon_P = \left(\frac{1 + 20Nb_{eff}}{6360}\right) d_0^{0.5} Z^{0.17} \quad (5)$$

where d_0 is the grain size at the start of a pass and Z is the Zenner–Hollomon parameter. The activation energy at the peak is reported to be 401.8 kJ mol^{-1} [27] thus Z could be expressed as below:

$$Z = \dot{\varepsilon} \exp\left(\frac{401800}{8.314\,T}\right) \quad (6)$$

where $\dot{\varepsilon}$ is strain rate and T is absolute temperature (K).

If softening fraction does not reach to 1 and recrystallization mechanisms partially occurs, some strains accumulate in the material from the previous passes that call retained strain (ε_r). Adding up the retained strain with the applying strain in each pass determines the accumulated strain (ε_a). The amount of the retained strain at beginning of each pass is a function of softening fraction and accumulated strain of the last passes that determined by the following relationships:

$$\varepsilon_r = \lambda(1 - X)\varepsilon_a \quad (7)$$

with $\lambda = 1$ if $X < 0.1$ and $\lambda = 0.5$ if $X \geq 0.1$, for Nb-microalloyed steels [15, 18, 28, 29]. Considering the statements for each pass of hot rolling there is:

$$\varepsilon_{a,i+1} = \varepsilon_{i+1} + \varepsilon_{r,i} = \varepsilon_{i+1} + \lambda(1 - X_i)\varepsilon_{a,i} \quad (8)$$

where i defines the ith pass of the hot rolling process. Equation 8 expresses that the deformation in each pass occurs by summation of the applying strain in that pass and the retained strain from the previous passes. Commonly, the applying strain in each pass practically is lower than the critical strain but due to the retained strain, the accumulated strain reaches to critical strain or even higher values.

In order to find which softening mechanism occurs in an inter-pass time, a comparison between accumulated strain and critical strain should be applied. If $\varepsilon_a < \varepsilon_c$ then SRX takes place else MDRX happens. When SRX occurs between passes $t_{0.5,SRX}$ describes as below [19]:

$$t_{0.5,SRX} = (-5.24 + 550[Nb_{eff}]) \times 10^{-18}\varepsilon_a^{-4+77[Nb_{eff}]}d_0^2 \exp\left(\frac{330000}{8.314\,T}\right) \quad (9)$$

On the other hand, if $\varepsilon_a > \varepsilon_c$ DRX is initiated during the deformation and MDRX takes place in inter-pass time. In this case the following relationship determines $t_{0.5,MDRX}$ [25]:

$$t_{0.5,MDRX} = 4.42 \times 10^{-7}\dot{\varepsilon}^{-0.59} \exp\left(\frac{153000}{8.314\,T}\right) \quad (10)$$

The grain size after full static recrystallization observed in a number of Nb-microalloyed steels has been shown to be a function of strain and initial grain size as follows [30]:

$$d_{SRX} = D\varepsilon^{-0.67}d_0^{0.67} \quad (11)$$

where the value of the constant D varies in the range 0.9–1.9 [26]. In this investigation the value of D is selected to be 1.1 as reported by Sellars [28].

The grain size after complete MDRX evaluates from [25]:

$$d_{MDRX} = 1370\left[\dot{\varepsilon}\exp\left(\frac{375000}{8.314\,T}\right)\right] \quad (12)$$

An interesting feature of this equation is that the recrystallized grain size does not depend at all on the original grain size.

In the case of incomplete recrystallization, the initial grain size for the following pass ($d_{0,i+1}$) can be calculated using the Eq. 13 [31–33] which specifies a kind of *average* derived from the freshly formed and original grain sizes:

$$d_{0,i+1} = X_i^{\frac{4}{3}}d_{RX,i} + (1 - X_i)^2 d_{0,i} \quad (13)$$

With this formulation, when X_i is close to 1, the initial grain size for the following pass is equal to recrystallized grain size, $d_{RX,i}$. On the other hand, if X_i is small, $d_{0,i+1}$ will be close to the original grain size, $d_{0,i}$; in the latter case, the grains only change their shapes because of the applied strain [31].

Afterwards static or metadynamic recrystallization completes, the equiaxed austenite microstructure coarsens by grain growth. In the multi-pass hot rolling, at least there is a very short interval time between the passes that the material takes no deformation. Some of this time is used for recrystallization and if there is any rest of the time, it would be used for grain growth. Therefore, each part of the inter-pass time should be denoted and calculated separately. Generally it is assumed that when 95% of recrystallization has done, the recrystallization is over and grain growth starts. With this assumption and by considering to Eq. 1, the recrystallization finishing time, t_{RXF}, can be calculated for SRX and MDRX which results in following equation:

$$t_{GG} = t_{ip} - t_{RXF} = t_{ip} - (4.322 \times t_{0.5}) \quad (14)$$

where t_{GG} is the time that material uses for grain growth after SRX and MDRX and t_{ip} is the inter-pass time. The grain size of coarsened grains for Nb-microalloyed steels given by Hodgson et al. [19, 34] is:

$$d_{0,i+1}^{4.5} = d_{RX,i}^{4.5} + 4.1 \times 10^{23}t_{GG,i}\exp\left(-\frac{435000}{8.314\,T}\right) \quad (15)$$

where t_{GG} is calculated from Eq. 14.

The other phenomenon which can be took place is strain induced precipitation of carbonitrides that effectively stops recrystallization or lead to retardation on it. Abad et al. [8] established that the precipitation needed to reach 5% completion in order to be effective to prevent recrystallization. Once the precipitation is started there would be no further recrystallization. A model to predict the start of precipitation in Nb-microalloyed steels has been proposed by Dutta and Sellars [35], shortened as DS model. Siciliano et al. [36] in another research concluded that DS model needs a revision for steels with additions of Mn and Si. Equation 16 would be used for calculation of precipitation start time, t_{ps}:

$$t_{ps} = \frac{A}{[Nb]\varepsilon_a Z^{0.5}}\exp\left(\frac{270000}{8.314\,T} + \frac{2.5 \times 10^{10}}{T^3(\ln(K_s))^2}\right) \times 10^{0.26+0.9[Mn]-2.85[Si]} \quad (16)$$

where A is a constant and K_s is supersaturation ratio proposed by Irvine et al. [37] which determined the "driving force" for precipitation. The value of A can be obtained by [5]:

$$A = \frac{\left(\frac{[Mn]}{[Si]}\right)^{0.42}\exp\left(\frac{0.42[Nb]}{[C]}\right)}{169400} \quad (17)$$

Also K_s is corrected by Siciliano and Jonas [5]. In order to make it easier to use, the value of $\ln(K_s)$ is simplified as follows:

$$\ln(K_s) = \left(\frac{1}{T} - \frac{1}{T_{rh}}\right) \times \left(1929.57[\mathrm{Mn}]^{0.246} - 2928.47[\mathrm{Si}]^{0.594} - 14828.65\right) \quad (18)$$

The last matter which should be considered here is the case of occurrence of precipitation before recrystallization finishing and having t_{ip} longer than t_{ps}. In order to handle it three conditions should be checked:

I: $t_{ip} < t_{ps}$
II: $t_{RXF} < t_{ps}$
III: $t_{RXS} < t_{PS}$

where t_{RXS} and t_{RXF} imply the meaning of recrystallization starting and finishing times, respectively. Assuming 5 and 95% of recrystallization as an indication of initializing and finalizing of recrystallization and using Eq. 1, following equation should be used to calculate the values of t_{RXS} and t_{RXF}:

$$t_{RXF} = 4.322 \times t_{0.5} \quad (19)$$

$$t_{RXS} = 0.074 \times t_{0.5} \quad (20)$$

Since the values of t_{RXS} and t_{RXF} differ with the mechanism of recrystallization, it is impossible to check conditions II and III at the very first step of calculations of microstructural evolution as Liu et al. [38] assumed for their work. In order to deal with this problem conditions I, II, and III should be checked in different steps of the prediction algorithm (Fig. 1). It should be noted that at the first step there is not any information about whether SRX occurs or MDRX.

Multi-pass flow stress curves

In this investigation, the material never experiences strains above the peak strain. The stress–strain behavior up to the peak has been modeled using an equation proposed by Solhjoo [39]:

$$\sigma = \sigma_P \left[\frac{\varepsilon}{\varepsilon_P}\left(2 - \frac{\varepsilon}{\varepsilon_P}\right)\right]^S \quad (21)$$

where σ_P is the peak stress and S is a constant. Using the flow curves in literature [40] for Nb-microalloyed steels the value of constant S is obtained to be 0.33.

The prominent dependence of the flow stress on the temperature and strain rate suggests that the hot deformation process is controlled by a thermally activated process, and the relation between these parameters is expressed by the following equation [41]:

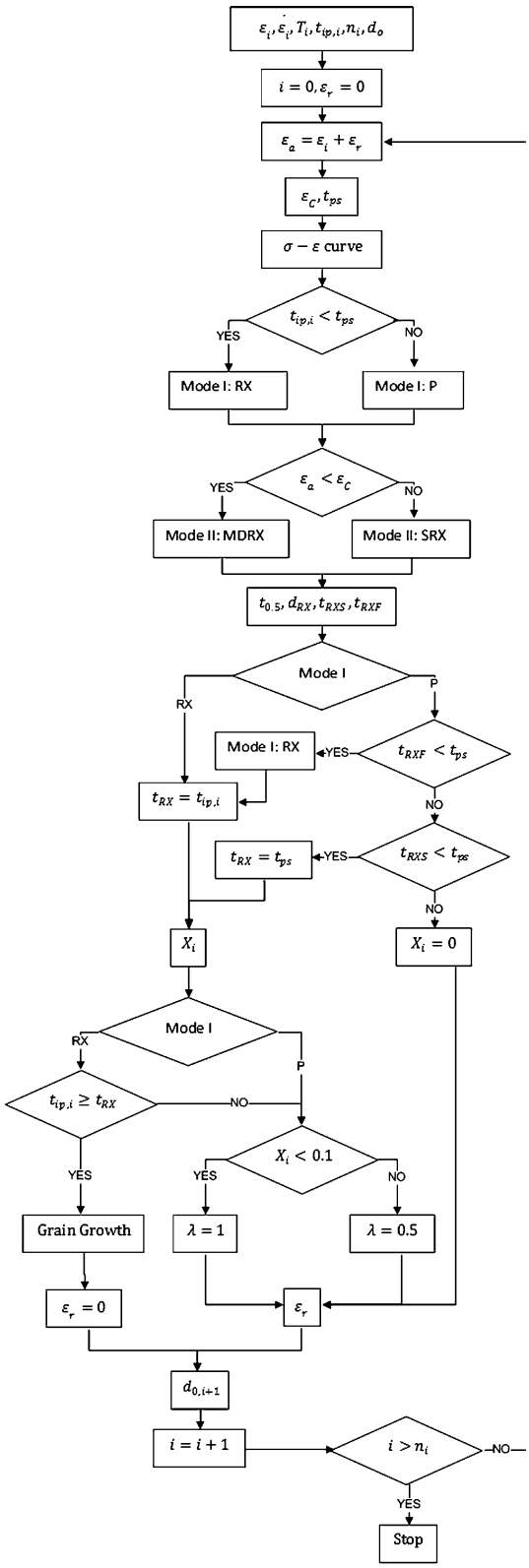

Fig. 1 Flow chart for calculating the microstructural evolution and multi-pass flow stress

$$\dot{\varepsilon} = A\sigma^m \exp\left(-\frac{Q_{\text{def}}}{RT}\right) \quad (22)$$

where A and m are constants, Q is the hot deformation activation energy, and R is the universal gas constant. The values of m and Q are reported to be 6.3 and 401.8 kJ mol^{-1}, respectively [27]. The value of A does not affect the value of computed T_{nr} but it found to be 6500 by trial and error. Thus the Eq. 22 for Nb-microalloyed steels changes into:

$$\dot{\varepsilon} = 6500\sigma_{\text{P}}^{6.3} \exp\left(-\frac{401800}{8.314\,T}\right) \quad (23)$$

Using this model the plastic behavior of the alloy can be found in a range of strain which is lower than the peak strain. The flow chart describing the algorithm which is used to predict the microstructural evolution and multi-pass flow stress curves is displayed in Fig. 1. n_i in the algorithm is the number of passes of the schedule. All 10 different hot torsion schedules presented in literature [42] (see Table 1) is simulated for 13 passes. Figure 2 shows a typical multi-pass flow stress curves obtained from the simulation at a strain rate of 2 s^{-1}, 0.35 pass strain and 30 s inter-pass time.

Experimental procedure

Experimental procedure and results were quoted from the literature [42]. A Nb-microalloyed steel was studied with the chemical composition of (in mass%) 0.11C, 0.11Si, 1.0Mn, 0.03Al, 0.034Nb, <0.004P, 0.0029S, 0.005O, and 0.0038N. Multi-pass hot torsion tests were employed to determine the T_{nr}. The torsion specimens had a gauge length of 22.4 mm and a diameter of 6.3 mm. The experiments were conducted using a servo-hydraulic, computer controlled MTS torsion machine. Low pass strains (0.2 and 0.35) were adopted in order to avoid the occurrence of dynamic recrystallization. For a particular test, the pass strain rate (2 s^{-1}) and inter-pass time (in the range from 20 to 200 s) were held constant. The selected temperature of first pass was 1180 °C. The average cooling rates during each inter-pass time in the different tests was 30 °C. The initial austenite grain size after reheating (at 1230 °C for 900 s) was large with an average size of 365 μm.

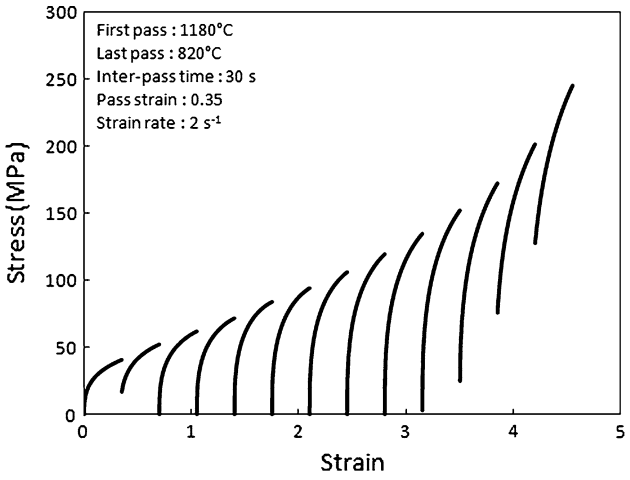

Fig. 2 Simulated stress–strain curve for thirteen-pass hot rolling test

Results and discussions

The determination of the no-recrystallization temperature is an important step in designing controlled rolling schedules. The value of T_{nr} can be determined from the variation of the mean flow stress (MFS) with inverse of the absolute temperature at which the deformation took place [10–16]. The method was developed by Jonas and co-workers [7] based on multi-pass torsion tests performed under continuous cooling conditions which needs complicated equipments. In this investigation an algorithm is used to simulate the flow stress curves for multi-pass hot deformation processes simply from the data of single-pass hot torsion/compression test which needs simple equipments.

The MFS is calculated as the area under a given stress–strain curve normalized by the strain. Therefore, the MFS between strains ε_1 and ε_2 is calculated as follows:

Table 1 T_{nr} and error values for steel used, determined be 13 passes hot rolling simulation from 1180 to 820 °C and inter-pass temperature of 30 °C

t_{ip} (s)	$\varepsilon = 0.2$					$\varepsilon = 0.35$				
	20	30	60	100	200	20	30	60	100	200
$T_{\text{nr}}^{\text{Ex}}$(K) [37]	1234	1255	1250	1220	1213	1201	1223	1213	1183	1173
$T_{\text{nr}}^{\text{Pr}}$(K)	1236	1254	1249	1227	1216	1197	1215	1220	1190	1191
$\lvert\Delta T_{\text{nr}}^{\text{Ex-Pr}}\rvert$(K)	2	1	1	7	3	4	8	7	7	18
Error	0.2	0.1	0.1	0.6	0.2	0.3	0.7	0.6	0.6	1.5

Strain rate=2 s^{-1}; reheating conditions: 1230 °C, 900 s

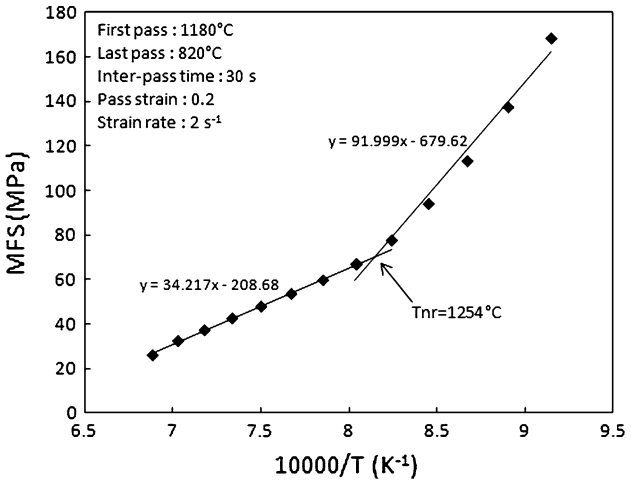

Fig. 3 MFS versus inverse absolute temperature

$$\text{MFS} = \bar{\sigma} = \frac{1}{\varepsilon_2 - \varepsilon_1}\int_{\varepsilon_1}^{\varepsilon_2} \sigma \mathrm{d}\varepsilon \tag{24}$$

The MFS for each pass is calculated using Eq. 24 and then the MFS plotted verses 10000/T. Figure 3 shows one of this plots for a strain rate of 2 s^{-1} and pass strain equal to 0.2 with 100 s inter-pass time. These plots can be divided into two ranges: a high temperature, lower slope region in which full recrystallization takes place and a low temperature, higher slope one in which only partial or no recrystallization takes place. By fitting straight lines to these two segments, a point of intersection is obtained, which is defined as the T_{nr} [21, 42].

By means of the method described for determination of T_{nr}, at the first place the multi-pass flow stress curves are simulated. Then the MFS is plotted versus 10000/T for all 10 different hot torsion schedules and the values of T_{nr} are determined. These values are compared to the experimental values in Table 1. The error of the predicted T_{nr} (T_{nr}^{Pr}) with experimental ones (T_{nr}^{Ex}) is calculated by the following equation:

$$\text{Error} = \frac{\left|T_{nr}^{Pr} - T_{nr}^{Ex}\right|}{T_{nr}^{Ex}} \times 100 \tag{25}$$

with absolute temperatures (K). Minimum and maximum errors in this estimation are 0.1 and 1.5%, respectively; which are very low values.

The effects of inter-pass time and pass strain on the T_{nr} values are illustrated in Fig. 4 obtained from the simulation. For times ranging from 20 to 200 s, the diagram can be divided into two regions: precipitation and precipitate coarsening [42]. In the precipitation region, the T_{nr} increases with inter-pass time until, after a certain time, the T_{nr} starts to decrease (precipitate coarsening). Also, the T_{nr} drops with increasing pass strain. It is reported that increasing the pass strain appears to accelerate the recrystallization kinetics more than the precipitation kinetics [42].

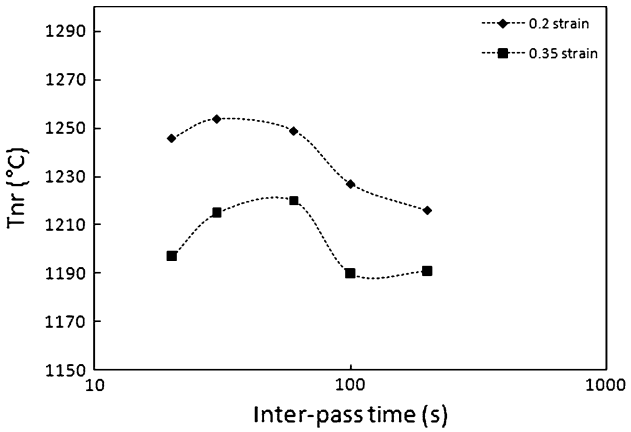

Fig. 4 Dependence of T_{nr} on inter-pass time for two different pass strains

Using the simulation tests, the effect of strain rate on T_{nr} is predicted in this investigation. For these tests, the inter-pass time was held constant at 30 s which shows the maximum value of T_{nr} [42]. The dependences displayed can be presented in the form [43]:

$$T_{nr} \alpha \dot{\varepsilon}^m \tag{26}$$

where m is a constant. The value of m is calculated to be 0.0004 and −0.0001 for pass strain of 0.2 and 0.35, respectively. As can be seen, the strain rate exponent has a very low value and it can thus be concluded that strain rate does not have a large influence on either the T_{nr} as reported in a previous research [43]. In addition, the influence of strain rate on recrystallization kinetics is too small [44].

Conclusions

In order to estimate the value of T_{nr} an algorithm is made which predicts the microstructural evolution and flow stress curves during multi-pass hot rolling processes. This goal is achieved by using single-pass hot torsion/compression test results. The flow stress curves for different hot rolling schedules are simulated and then using the plot of MFS verses 10000/T the values of T_{nr} are calculated for each schedule. Maximum error in calculation of T_{nr} with this method and the values obtained from empirical tests was 1.5%.

References

1. Gómez M, Medina SF, Quispe A, Valles P (2002) ISIJ Int 42:423
2. Bain EC, Paxton HW (1961) Alloying elements in steel ASM. Metals Park, Ohio

3. Yue S, Jonas JJ (1990) Mater Forum 14:245
4. Teoh LL (1995) J Mater Process Technol 48:475
5. Siciliano F, Jonas JJ (2000) Metall Mater Trans A 31:511
6. Vega MI, Medina SF, Chapa M, Quispe A (1999) ISIJ Int 39:1304
7. Bai DQ, Yue S, Sun WP, Jonas JJ (1993) Metall Trans A 24:2151
8. Abad R, Fernandez AI, Lopez B, Rodriguez-Ibabe JM (2001) ISIJ Int 41:1373
9. Maccagno TM, Jonas JJ, Yue S, McCrady BJ, Slobodian R, Deeks D (1994) ISIJ Int 34:917
10. Najafi-Zadeh A, Yue S, Jonas JJ (1992) ISIJ Int 32:213
11. Medina SF, Vega MI, Chapa M (2000) Mater Sci Technol 16:163
12. Samuel FH, Yue S, Jonas JJ, Zbinden BA (1989) ISIJ Int 29:878
13. Pussegoda LN, Jonas JJ (1991) ISIJ Int 31:278
14. Samuel FH, Yue S, Jonas JJ, Barnes KR (1990) ISIJ Int 30:216
15. Karjalainen LP, Maccagno TM, Jonas JJ (1995) ISIJ Int 35:1523
16. Kojima A, Watanabe Y, Terada Y, Yoshie A, Tamehiro H (1996) ISIJ Int 36:603
17. Semiatin SL, Lahoti G, Jonas JJ (1985) ASM metals handbook, vol 8 (mechanical testing) 9th ed ASM. Metals Park, Ohio
18. Sellars CM, Whiteman JA (1979) Met Sci 13:187
19. Hodgson PD, Gibbs RK (1992) ISIJ Int 32:1329
20. Fernández AI, Uranga P, López B, Rodriguez-Ibabe JM (2000) ISIJ Int 40:893
21. Uranga P, Fernández AI, López B, Rodríguez-Ibabe JM (2004) ISIJ Int 44:1416
22. Roucoules C, Hodgson PD, Yue S, Jonas JJ (1994) Metall Trans A 25:389
23. Sellars CM (1980) In: Sellars CM, Davies GJ (eds) Hot working and forming processes. Met Soc, Institute of Materials, London
24. Xu YB, Yu YM, Xiao BL, Liu ZY, Wang GD (2010) J Mater Sci 45:2580. doi:10.1007/s10853-010-4229-6
25. Roucoules C (1992) Dynamic and metadynamic recrystallization in HSLA steels. PhD Thesis, McGill University Montreal
26. Minami K, Siciliano F, Maccagno TM, Jonas JJ (1996) ISIJ Int 36:1507
27. Ouchi C, Okita T (1982) Trans ISIJ 22:543
28. Sellars CM (1990) Mater Sci Technol 6:1072
29. Park SH, Yue S, Jonas JJ (1992) Metall Trans A 23:1641
30. Jonas JJ (1994) Mater Sci Eng A 184:155
31. Maccagno TM, Jonas JJ, Hodgson PD (1996) ISIJ Int 36:720
32. Maccagno TM, Jonas JJ (1994) ISIJ Int 34:607
33. Beynon JH, Sellars CM (1992) ISIJ Int 32:359
34. Pietrzyk M, Roucoules C, Hodgson PD (1995) ISIJ Int 35:531
35. Dutta B, Sellars CM (1987) Mater Sci Technol 3:197
36. Siciliano F, Maccango TM, Nelson BD, Jonas JJ (1997) In: Chandra T, Sakai T (ed) Thermec '97, TMS, Warrendale
37. Irvine KJ, Pickering FB, Gladman T (1967) J Iron Steel Inst 205:161
38. Liu XD, Solberg JK, Gjengedal R, Kluken AO (1994) J Mater Process Technol 45:497
39. Solhjoo S (2010) Mater Des 31:1360
40. Beladi H, Hodgson PD (2007) Scripta Mater 56:1059
41. Sellars CM, McG Tegart WJ (1966) Mem Sci Rev Metall 63:731
42. Jiang L, Humphreys AO, Jonas JJ (2004) ISIJ Int 44:381
43. Bai DQ, Yue S, Maccagno T, Jonas JJ (1996) ISIJ Int 36:1084
44. Laasraoui A, Jonas JJ (1991) Metall Trans A 22:151